Climate Dynamics (1998) 14:213–231

K. E. Trenberth · C. J. Guillemot

Evaluation of the atmospheric moisture and hydrological cycle in the NCEP/NCAR reanalyses

Received: 28 October 1996 / Accepted: 11 September 1997

Abstract An evaluation is carried out of the moisture fields, the precipitation P and evaporation E, and the moisture transport and divergence in the atmosphere from the global atmospheric National Centers for Environmental Prediction (NCEP)–NCAR reanalyses produced with four-dimensional-data assimilation. The moisture fields are summarized by the precipitable water which is compared with analyzed fields from NVAP based primarily on Special Sensor Microwave Imager (SSM/I) over the oceans and rawinsonde measurements over land, plus TIROS Operational Vertical Sounder (TOVS). The moisture budgets are evaluated through computation of the freshwater flux at the surface $E - P$ from the divergence of the total moisture transport, and this is compared with the reanalysis $E - P$ that is based upon a 6-hour integration of the assimilating model and thus depends on the model parametrizations. The P field is evaluated using Xie–Arkin global precipitation estimates which, although containing considerable uncertainties, are believed to be reliable and good enough to show that there are substantial biases in the NCEP P. There are many fields of interest and which are improved over previous information available. On an annual mean basis the largest evaporation of over 6 mm/day is in the subtropical Indian Ocean. However, the NCEP moisture fields are shown to contain large and significant biases in the tropics. The tropical structures are less well defined and values are generally smaller where they should be high and higher where they should be low. In addition, the NCEP moisture fields contain less variability from year to year. The NCEP model P generally reveals a double intertropical convergence zone in the central Pacific and the location of the South Pacific Convergence Zone is not well captured. Rainfall amounts are lower than observed in the oceanic tropical convergence zones. The variability in the central tropical Pacific of P associated with El Niño-Southern Oscillation (ENSO) is underestimated in the NCEP reanalyses and, moreover, is not very well correlated with the Xie–Arkin product. A bias for too much rainfall in the model over the southeastern USA and southeast Asia is also present in northern summer. The comparison of $E - P$ from the moisture budget with the model results reveal some strong systematic differences. In particular, remarkably, many island stations show up as bull's-eyes in the difference field. These are identified as originating from small but systematic differences in vertical moisture profiles from those in the surrounding oceans, raising questions about the influence radius of rawinsonde moisture observations. Biases in E are inferred from the $E - P$ differences in some places implying some spurious land moisture sources. While usually better, the residual method $E - P$ estimates are inferior to those from the model parametrizations in some places. Both estimates are affected by biases in moisture, as analyzed, and the moisture divergence depends critically on the velocity divergence field. The model estimates also depend upon the parametrizations of subgrid scale processes, such as convection, that influence E and P. A discussion is given of sources of errors contributing to the moisture budgets.

K. E. Trenberth (✉) · C. J. Guillemot
National Center for Atmospheric Research, PO Box 3000, Boulder, CO 80307, USA
E-mail: trenbert@ncar.ucar.edu

1 Introduction

Moisture is critically important to life on Earth. It also plays an important role in the heat budget of planet Earth especially through the greenhouse effect of water vapor and, at the surface, by moderating surface temperature changes as heating goes into evaporating moisture rather than increasing temperature. In addition, the transport of water vapor by the

atmosphere effectively redistributes the latent heat. Yet only recently has attention been given to improving moisture fields in global analyses and weather forecasting.

Reasons for the scanty knowledge of both moisture in the atmosphere and precipitation stem from the lack of observations, especially over the oceans, and their spatio-temporal variability. Rainfall and clouds often occur on quite small time and space scales, so that a single moisture or precipitation observation may not be representative of more than an area with dimensions of a few kilometers across or for more than a small fraction of a day. Experience with atmospheric models indicates that they quickly adjust the moisture fields to be compatible with the model moist physics, of which moist convection is probably the most critical. Therefore, in the past, observed information has not proven to be very valuable in numerical weather prediction and there has been little incentive to ensure that the information is utilized to the full, although research has begun in several places to redress this deficiency. Moreover, it follows that moisture fields from four dimensional data assimilation (4DDA) may not be very good estimates of the real world.

Measurements of accumulated precipitation are available in relatively widely spaced locations only where humans live, and the buckets used to measure accumulations may not catch it all, especially under snowy and windy conditions (Legates and Willmott 1990). Satellite measurements of moisture have been made available to the global analyses from TOVS (TIROS Operational Vertical Sounder), although with mixed results (Liu et al. 1992; Wittmeyer and Vonder Haar 1994). After July 1987 fields of precipitable water and other quantities from the Special Sensor Microwave Imager (SSM/I) have become available, but may not be used operationally. Recently, a special set of global analyses of water vapor has been compiled taking advantage of the radiosonde measurements combined with SSM/I and TOVS data called NVAP (Randel et al. 1996). Also, a number of different data sources are being utilized to put together global monthly mean fields of precipitation through the Global Precipitation Climatology Project (GPCP) (Huffman et al. 1997) for the period after 1987 and these are extended to cover the period after 1979 by Arkin and Xie (1994) and Xie and Arkin (1996, 1997) and called the Climate Prediction Center (CPC) Merged Analysis of Precipitation (CMAP). Over land these fields are mainly based on information from rain-gauge observations, while over the ocean they primarily use satellite estimates made with several different algorithms based on outgoing longwave radiation (OLR), and scattering and emission of microwave radiation. Because the latter consist of an integration of spot estimates of precipitation rate, they are subject to considerable sampling uncertainties. In some regions, such as the Intertropical Convergence Zone (ITCZ) in the Pacific, results from these algorithms do not agree very well, and so uncertainty exists as to the true values (e.g., Chiu et al. 1993). In addition, there remain gaps where there is insufficient information from either in situ or satellite-based measurements to provide monthly mean precipitation, yet it is highly desirable for many purposes to have complete fields. Accordingly, Xie and Arkin (1996, 1997) use the National Centers for Environmental Prediction (NCEP)-NCAR reanalysis P to fill the gaps which exist, mainly over the Arctic and southern oceans, and this will limit the value of the comparison with the NCEP/NCAR product. Nevertheless, we will use the NVAP and Xie–Arkin (CMAP) results as one version of "truth." Alternative estimates of these fields come from the assimilating model used in 4DDA, usually from a short model integration, but their evaluation using other sources is a primary purpose of this study.

Other quantities related to moisture and its sources and sinks are less well known. Trenberth and Guillemot (1995) evaluated the precipitable water and moisture budgets from the global analyses of European Centre for Medium Range Weather Forecasts (ECMWF), the US National Meteorological Center (NMC) (now NCEP) and NASA/Goddard and examined the differences between evaporation E and precipitation P, $E - P$, from 1987 to 1993. The precipitable water from the global analyses was computed and compared with satellite data from the SSM/I. Fluxes of moisture and their divergence were used to estimate the vertically integrated moisture budget and thus $E - P$ as residuals. Here we use a similar approach but with the NCEP/NCAR (henceforth NCEP) reanalyses (Kalnay et al. 1996) and use will be made of the analyses in model (sigma) coordinates at full resolution thereby avoiding any errors in interpolating to pressure surfaces and allowing exact vertical integrals to be computed. The mean and variability of the NCEP reanalysis fields of column integrated moisture and $E - P$ are assessed using the datasets outlined as well as indirect estimates using budget methods. Full results have been presented in an atlas form (Trenberth and Guillemot 1996) as means, differences, and standard deviations and only a small subset are presented here.

All of the fields are available from NCAR. These include the monthly, seasonal, and annual fields, as well as the summary statistics. Please access the World Wide Web at **http://www.cgd.ucar.edu/cas/catalog/tn430/** for a catalog of the datasets and check out the Climate Analysis Section (CAS) homepage for access to publications. The fields are all available through anonymous ftp accessible through this web site.

2 Computations and methods

Trenberth (1997) describes possible methods for estimating surface fluxes including (1) use of bulk fluxes and in situ observations, (2) use of model parametrizations to interpret specified inputs and compute

surface fluxes, and (3) various indirect methods. The latter rely on the fact that the mass and surface heat, energy, and momentum budgets must balance. Then, given computations of all the other components in the various budget equations applied to fields either within the ocean or the atmosphere, fluxes may be inferred as a residual. Trenberth (1997) reviews the third approach using indirect methods and outlines the advantages associated with the use of global atmospheric analyses from 4DDA. The time mean of the analysis increment arising from producing the analyses in 4DDA is identical to the systematic short-term (6 h) assimilating-model forecast error and is most likely due to errors in the model physics. Therefore the analyses include a desirable fix which allows the sum of the "physics" to be deduced from the "dynamics".

The second method arises naturally out of 4DDA. Atmospheric GCMs are used as part of 4DDA systems, and the model can be used along with the analyses to provide surface fluxes as a derived outcome from the model parametrizations. For some fluxes, this requires a short integration. Thus products from the reanalyses include estimates of evaporation E and precipitation P, but they are "C- variables" (to use the NCEP terminology) which are generated entirely by the model used in the 4DDA. They therefore depend heavily on the often uncertain formulae used and model parametrizations. Commonly a "spin up" occurs in the model in which a violent adjustment takes place, for instance in the divergence and/or moisture field, perhaps through a convective process, indicating an incompatibility between the observed and model-preferred states. Biases, such as manifested in climate drift or in systematic forecast error, would show up as errors in the derived fluxes. For example, it is vital to get an accurate shortwave radiation at the surface, but this depends critically on the cloud diagnosed in the model, and errors of several tens of $\mathrm{W\,m^{-2}}$ are common (see for instance Gleckler et al. 1995).

The NCEP system is based on a numerical weather prediction model with T62 spectral resolution and 28 levels in the vertical with five of those levels in the atmospheric boundary layer. The Spectral Statistical Interpolation (SSI) scheme is employed in the analysis with complex quality control. Fields are not initialized. A preliminary evaluation of some aspects of the NCEP reanalyses from the standpoint of moisture transport is given by Mo and Higgins (1996), although the main comparison is with reanalysis results from NASA/Goddard. They note that there is very little spinup between 0–6 h and 12–24 h forecast values of the NCEP model evaporation although there is some precipitation spin-up of 0.1 to 0.2 mm/day, with maxima in the tropics.

The global analyses are produced on model (sigma) surfaces which consist of a sigma (σ) terrain-following coordinate in which the lowest level corresponds to $p = p_s$, where p is pressure, p_s is the surface pressure and $\sigma = p/p_s$.

For water vapor, the conservation equation is

$$\frac{\partial w}{\partial t} + \nabla \cdot \frac{1}{g} \int_0^{p_s} q\,\mathbf{v}\,dp = E - P \qquad (1)$$

where the precipitable water $w = \frac{1}{g}\int_0^{p_s} q\,dp$, q is the specific humidity, E is the rate of evaporation and P is precipitation rate per unit mass, and we have ignored other forms of liquid and frozen water in the atmosphere.

All of the terms on the left hand side of Eq. (1) can be evaluated from the analyses, along with the implied $E - P$ as a residual. Vertical integrals for w and in Eq. (1) are evaluated using finite differences applied to the full model-level analyses. In addition, both terms on the right hand side of Eq. (1) can be computed from the 6-h integration with the assimilating model (the C variables). The differences between the two estimates of $E - P$ provide, in effect, a determination of the extent to which the moisture budget balances in the NCEP fields. Note that 6-h predicted values of w are not used.

We have carried out a systematic evaluation of the monthly, seasonal and annual fields by computing means, standard deviations and anomalies of NCEP precipitable water, model-based evaporation, precipitation and implied $E - P$, the vertically integrated flux of moisture (as a vector), the divergence of the latter, the tendency in moisture, $E - P$ from the moisture budget from the previous two quantities, and the differences between the two estimates of $E - P$. The evaporation is computed from the quantity archived as the surface latent heat flux. The base period for the climatology is 1979 to 1995. Similar statistics are computed from precipitable water from NVAP and P from Xie–Arkin CMAP, along with differences with the model-based values when available, so that we can thoroughly document the mean bias, the standard deviations of the differences (indicating the typical errors), and the correlation between the anomalies. For NVAP we are restricted to the more limited period from 1988 to 1992, and difference statistics with NVAP use only the common data. These calculations provide indications of whether the model-estimated anomalies are meaningful even if there are biases present in the total fields.

In computing tendencies, we define a month to consist of the observations during that month from 0000 UTC on the first day to 1800 UTC on the last day. Accordingly, the month actually is centered on the period from 2100 UTC on the last day of the previous month to 2100 UTC on the last day of the month in question. To compute the tendency of any quantity over this period, then requires a difference between values averaged as $0.5(V_{1800} + V_{0000})$ effective at 2100 on the last day of the month minus the same quantity the last day the previous month. Since files are arranged in months, it is worth noting that this requires information from not only the current month but also the previous and next month. Where standard deviations are computed, the division is by $N - 1$ rather than N, where N is the number of observations, in order to provide an unbiased estimate.

3 Evaluation of analyses

Results are presented here mainly for the annual means. Complete results are presented in the atlas by Trenberth and Guillemot (1996). All figures presented have been truncated to T31 and the contour interval is given immediately below each plot. The units are given at upper right. For seasons, conventional months are used grouped as December–January–February (DJF), March–April–May (MAM), June–July–August (JJA), and September–October–November (SON). Most plots contain side panels with the zonal mean values.

3.1 Precipitable water

Figures 1 and 2 show the annual mean precipitable water and its standard deviation, and thus how well the NCEP reanalyses replicate the NVAP fields which are believed to be quite an accurate depiction of the truth. Although the shortness of the NVAP record limits the comparison, the results reveal substantial shortcomings in the NCEP reanalyses. The differences between the NCEP w and the NVAP observations for their common period show the bias, while the standard deviations reveal their variability and possible biases in that variability. Very similar patterns are present in all months and seasons. Figure 3 shows the correlation between monthly anomalies (i.e., with mean annual cycle taken out) to indicate the extent to which the two fields covary. Although correlations between the two

fields are quite high, moisture is depleted in the tropical convergence zones by 4 to 12 mm, while too high in the South Pacific high. The tropical structures are less well defined in the NCEP reanalyses and values are generally smaller where they should be high and higher where they should be low, a pattern also present in earlier operational analyses (Trenberth and Guillemot 1995). In addition, the NCEP fields reveal less variability from year to year in analysed w in the tropical Pacific than in the NVAP data (Fig. 2). Dominant variations are found in the tropical Pacific in association with the El Niño-Southern Oscillation (ENSO) phenomenon, but the variances in the NCEP fields are especially deficient in the central and western tropical Pacific in all seasons.

Time series of anomalies (departures from the monthly means) of the NCEP precipitable water (Fig. 4) are given for the zonal mean, and meridional cross sections at 120 °E and 120 °W. These are presented to highlight the large ENSO-related variations that tend to have opposite signs at these two longitudes, while the zonal mean mostly reflects the values at 120 °W and is a consequence of the broad zonal extent of the anomalies in the central and eastern Pacific. Because of the cancellation, the zonal means are a small residual of the much larger values locally. Positive zonal mean anomalies >1 mm occur in 1982–83, 1987 and 1990–91 in the tropics, although at somewhat different latitudes. Negative anomalies <-1 mm occur in 1988–89 and late 1984. The negative anomalies in 1992 extend almost globally and are unique in that respect, and may be a consequence of the widespread cooling that occurred following the June 1991 Mount Pinatubo eruption (Jones 1994; Hurrell and Trenberth 1996).

3.2 Precipitation

Figures 5 and 6 show the annual precipitation field and its standard deviation from NCEP compared with the Xie–Arkin CMAP product. While the latter can not be considered to be fully quantitatively accurate (e.g., see Chiu et al. 1993), the patterns should be reasonable. There appear to be noteworthy biases in the NCEP P. The NCEP model P generally reveals a double intertropical convergence zone (ITCZ) in the central Pacific and the location of the South Pacific Convergence Zone (SPCZ) is therefore not well captured. Rainfalls are weak relative to the Xie–Arkin product in the ITCZ, but excessive over northern South America. A bias for too much rainfall in the model over the southeastern USA and also over southeast Asia is also present in northern summer (Fig. 7). The standard deviation maps (Fig. 6) reveal that the variability in the central tropical Pacific of P associated with ENSO is severely underestimated in the NCEP reanalyses, and moreover, is not very well correlated with the Xie–Arkin product (Fig. 8). The high variability over east Antarctica in the CMAP fields is spurious. In the correlation between the two P fields (Fig. 8), values exceed 0.8 only around Antarctica, in the Arctic, and in tropical eastern Pacific. In both of the polar oceans, the deficit of real data led to the substitution of NCEP P values in the Xie–Arkin analysis, and so the two products are dependent and should be closely related. This is not so in the tropical eastern Pacific, where an ENSO-related signal is apparently captured by the NCEP reanalyses. Elsewhere, correlations are mostly lower than 0.6 and approach zero in the tropical western Pacific.

In places where P is strong, especially the ITCZs, there is a low bias in model P. Thus the low bias in precipitable water in the tropics could be a factor in contributing to lower rainfall rates and, at the same time, lower rainfalls mean less latent heating and feedback to the divergent flow which transports the moisture into the region, thereby contributing to the biases in moisture amounts.

3.3 Moisture transports, moisture budget, and evaporation

Figure 9 shows the vertically-integrated total moisture transport for the annual mean and DJF and JJA seasons. It is noteworthy that the main moisture transports are east–west, with strong westward components in the tropics and eastward components in the middle latitudes, but the meridional components linking the two are much weaker. The main exception occurs in JJA with the Asian summer monsoon and then there is a strong northward flow from the Southern Hemisphere subtropics in the Somalian jet into India and southeast Asia. The corresponding northward flow in the low level jet from the Gulf of Mexico into the United States is quite small by comparison. The only other meridional moisture flux of consequence is just off the east coast of Brazil in the southern summer. The subtropical highs form the zones in between the main zonal transports and are the main sources of evaporation, especially in the winter. These patterns also reflect the total mean mass flux and the dominance of the easterlies and westerlies, thereby emphasizing the importance overall of the moisture transport by the mean flow.

The surface fresh water flux $E-P$ from the moisture budget residual calculation is given in Fig. 10 for the annual mean and its standard deviation. The locations of the dry subtropics and ITCZ are qualitatively well depicted by the side panels representing zonal averages of mean $E-P$. Maximum zonally-averaged values of $E-P$ of about 3 mm/day are observed in January near 20 °N while they reach 4 mm/day near 20 °S in July. Excess precipitation of 1.5 to 2.5 mm/day in the zonal mean is found near the equator in association with the

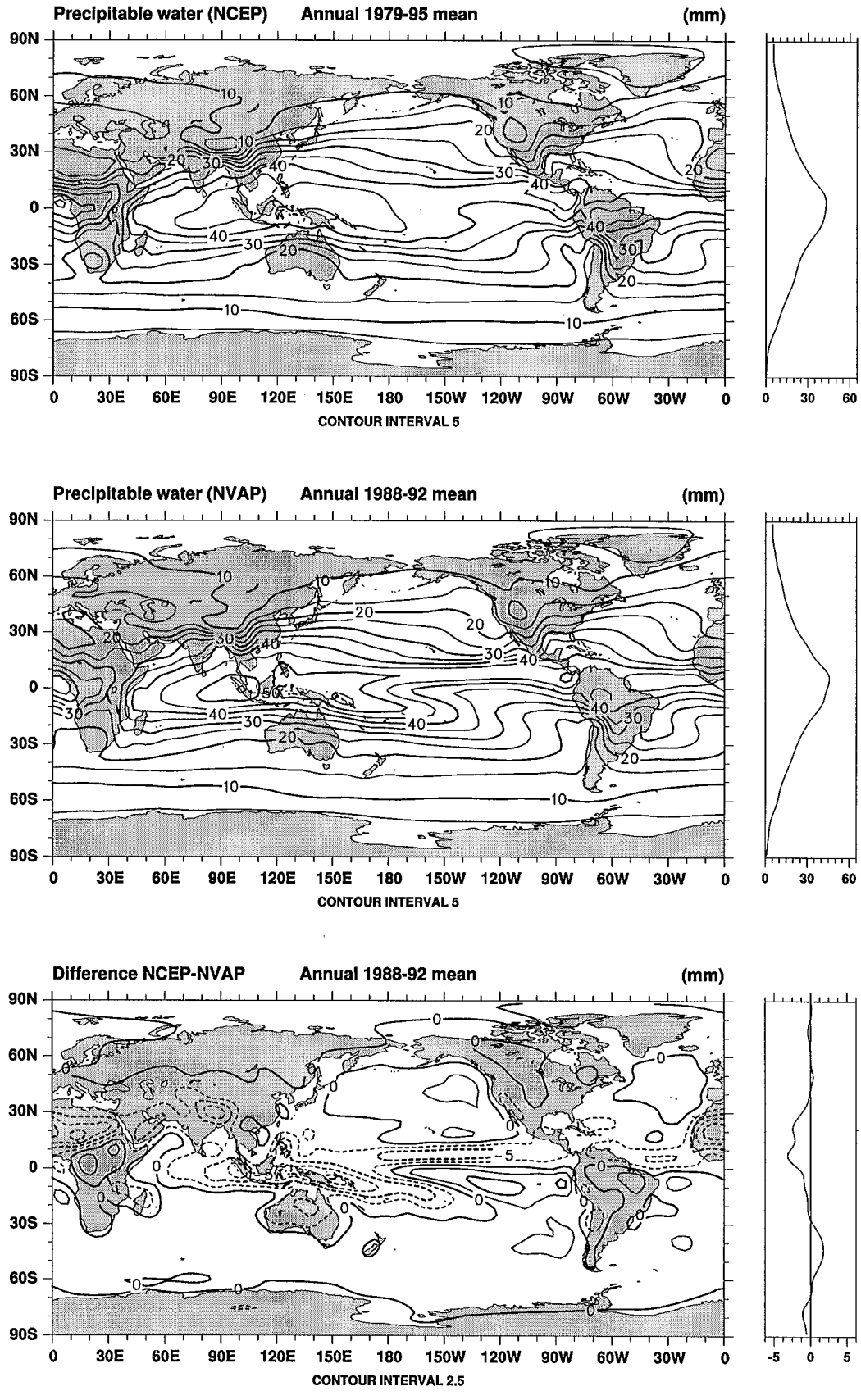

Fig. 1 Annual mean precipitable water for the period 1979–1995 (NCEP) and 1988–1992 (NVAP), and their differences based on 1988–1992. All quantities have been truncated to T31 for presentation in all figures, the contour interval is given below each plot and the units are at upper right. *Negative values* are *dashed*. *At right* the zonal mean meridional profile is given

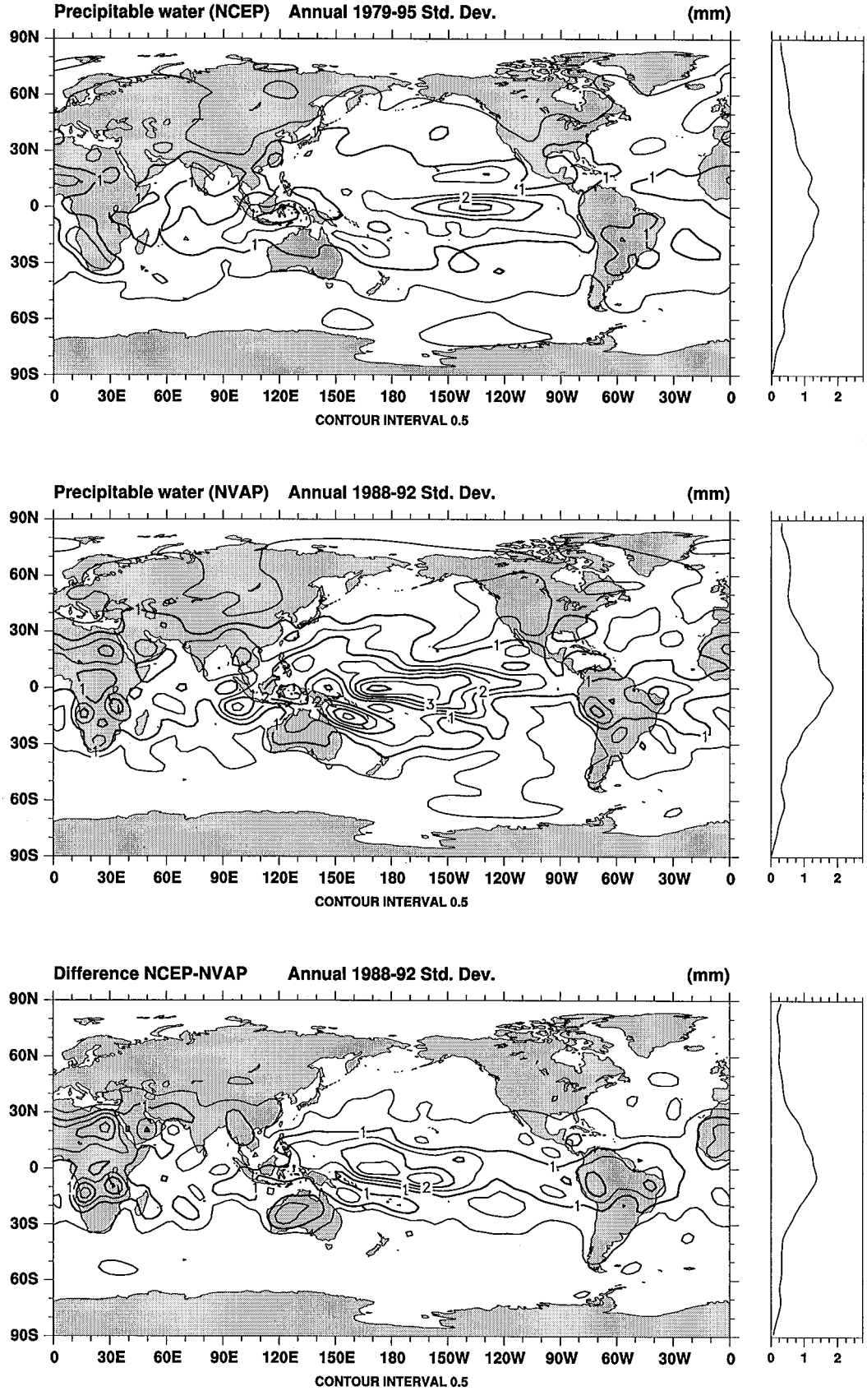

Fig. 2 Standard deviation of the annual mean precipitable water for the period 1979–1995 (NCEP) and 1988–1992 (NVAP), and the standard deviation of their differences for the common period

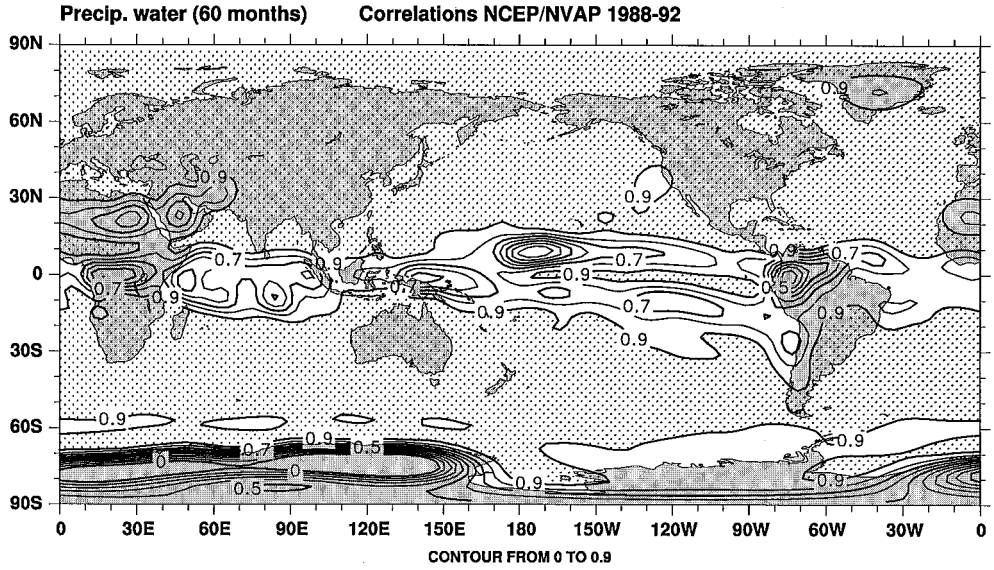

Fig. 3 Correlation coefficient between the monthly anomalies in precipitable water in NCEP and NVAP analyses over the period 1988 to 1992 (60 mon). *Values* exceeding 0.9 are *stippled* and only contours 0, 0.5 and at intervals of 0.1 above 0.5 are plotted

ITCZ and monsoonal rains in every month of the year, with a somewhat broader latitudinal extent of the peak during the northern winter located from 5 °N to 10 °S, while the northern summer minimum in $E - P$ is sharply peaked near 10 °N. Standard deviations of $E - P$ (Fig. 10) are largest in the tropics but do not appear to be very seasonally dependent. Seasonal and monthly values are substantially larger by factors of roughly $3^{\frac{1}{2}}$ for seasons and $12^{\frac{1}{2}}$ for months, as would be expected for monthly values that are independent. To the extent that these variations in $E - P$ can be believed, they provide a measure of the anomalies in the fresh water flux which alter the salinity of the ocean, and thus the buoyancy, and this is of interest especially for its potential to alter the thermohaline circulation.

The time series of variations in $E - P$ (Fig. 11) mostly reveal the annual cycle which was commented on already. The maxima in P and thus minima in $E - P$ occur in the summer of each hemisphere in the tropics while the strongest evaporation (maxima in $E - P$) occurs in the subtropics in winter. In the Northern Hemisphere there is a further minimum each winter north of 40 °N associated with the development of the storm tracks over the oceans and associated precipitation maximum. Over the maritime Southern Hemi sphere extratropics $P > E$ year round. There are only very small decadal variations in $E - P$ and even the interannual variability is always < 1 mm/day for the zonal mean owing to strong cancellation between much larger regional variations. The largest anomalies are ENSO related of 0.9 mm/day in DJF 1982–83 near 10 °N, and -0.3 mm/day from 0 to 15 °S. Similar anomalies of -0.3 mm/day from 5 °S to 10 °N occur in association with the 1987 ENSO event.

Figure 12 presents the evaporation E for the annual mean, the annual standard deviation and for DJF. During the northern winter the dry cold air spilling eastward over the Pacific from Asia gives rise to a very pronounced moisture and evaporation gradients over coastal waters. The same is true off the east coast of North America and, to a lesser extent, in the Indian Ocean as a result of the winter monsoon. On an annual mean basis the largest evaporation of over 6 mm/day is in the subtropical Indian Ocean, as was also found in ECMWF analyses (Trenberth and Solomon 1994). Smaller areas of similar magnitude occur over the East Australia current and Gulf Stream. Otherwise, the largest values of evaporation generally occur over the warm northward-flowing ocean currents in the western Pacific and Atlantic in winter. The more maritime Southern Hemisphere is characterized by a more zonal distribution of evaporation with the largest values found over subtropical waters. Note that the standard deviation is typically 0.2 to 0.3 mm/day over the oceans in the tropics and subtropics, and somewhat less over land, values which are much less, by a factor of 4 in the tropics, than the standard deviation of P. As noted by Trenberth and Guillemot (1995), the spatial and temporal variability of E is much less than that of P and so the latter dominates the variability of the fresh water flux $E - P$.

The divergence of the moisture flux accounts for the bulk of the $E - P$ quantity. The precipitable water tendency shown in Fig. 13 accounts for generally less than 3% of the $E - P$ product, but it is important in the transition seasons when the maximum in moisture systematically switches from one hemisphere to the other.

3.4 Differences between $E - P$ estimates

The computed differences between the two annual $E - P$ fields (Fig. 14) reveal the extent to which the

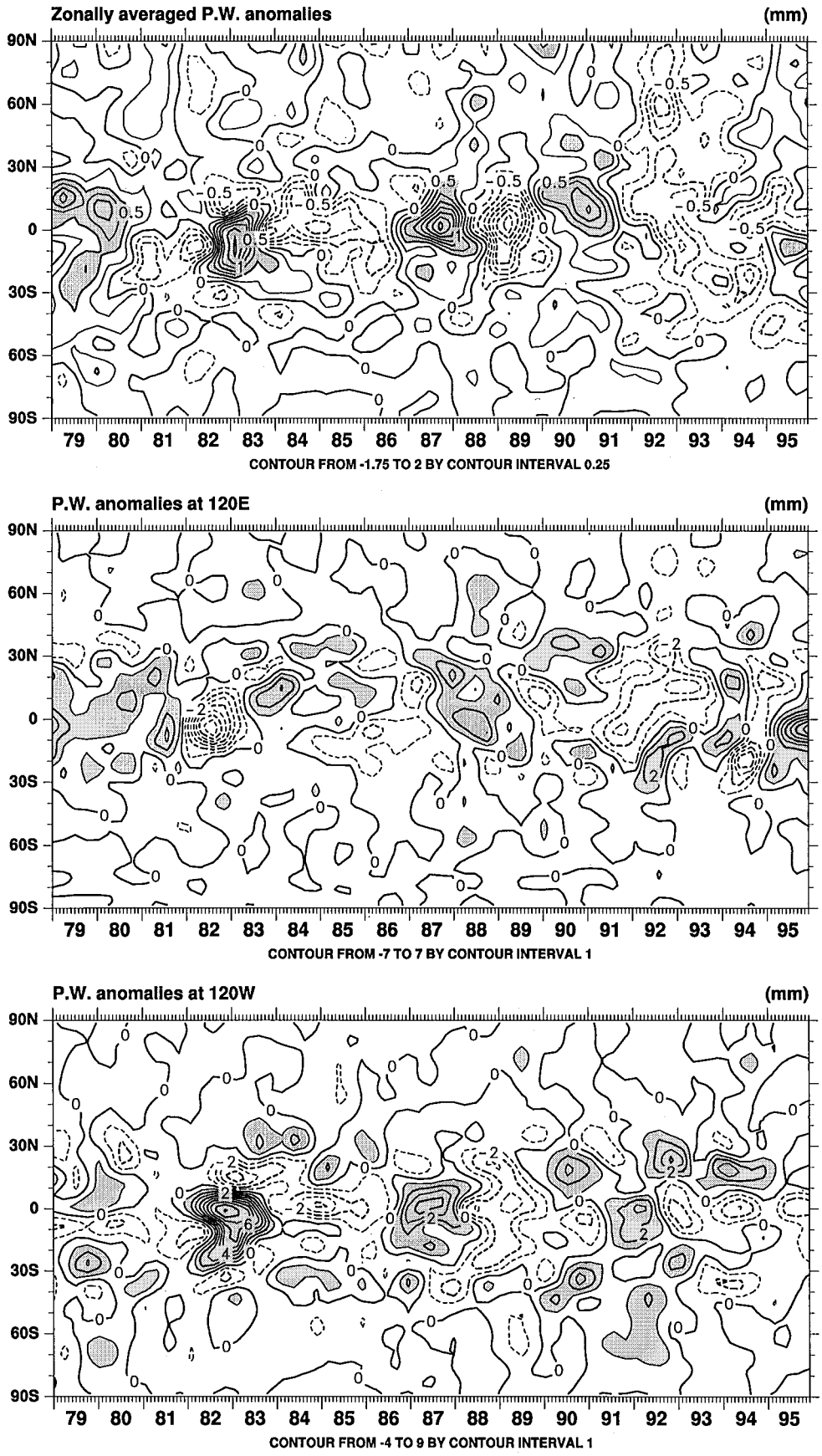

Fig. 4 Latitude-time series of monthly mean anomalies of *w* from the NCEP reanalyses for the zonal mean, 120 °E and 120 °W. All fields were first truncated at T31 and a 1–2–1 smoother has been applied to reduce noise. *Positive values* exceeding 0.5 mm (*top panel*) and 1 mm (*lower two panels*) are *shaded*

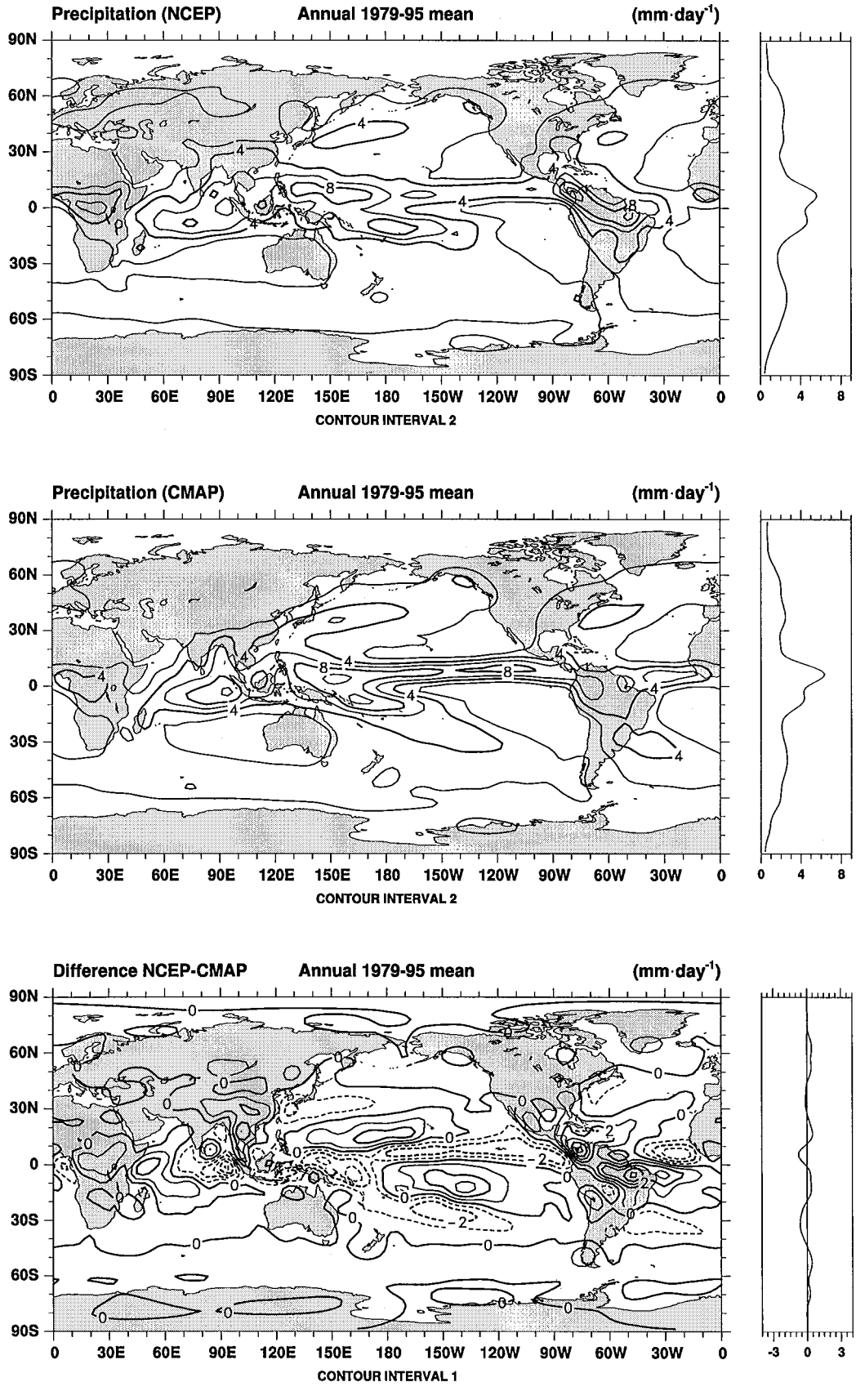

Fig. 5 Annual mean precipitation for the period 1979–1995 from the model, Xie–Arkin CMAP and their differences

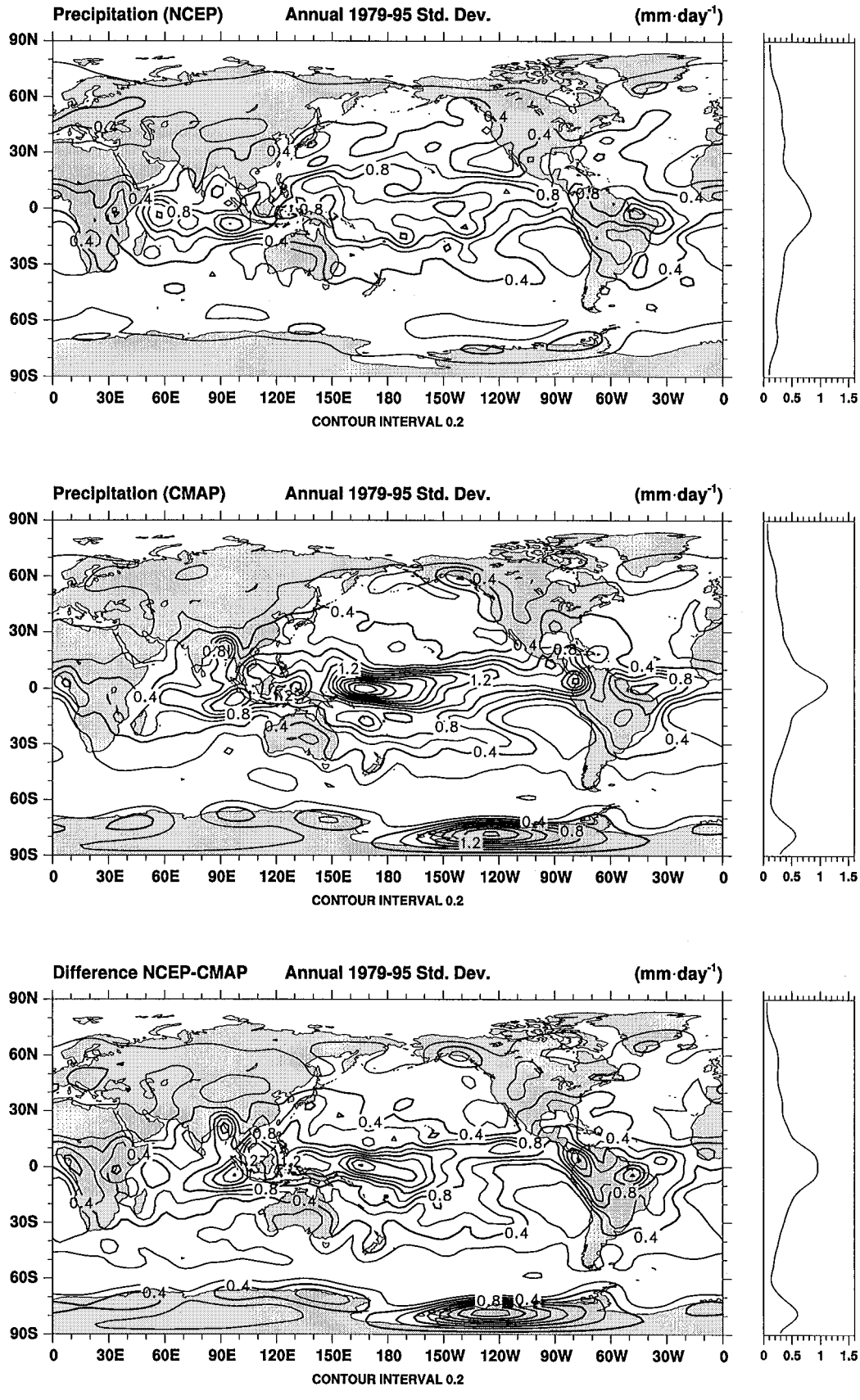

Fig. 6 Standard deviation of the annual mean precipitation for the period 1979–1995 from the model, CMAP and the standard deviation of their differences

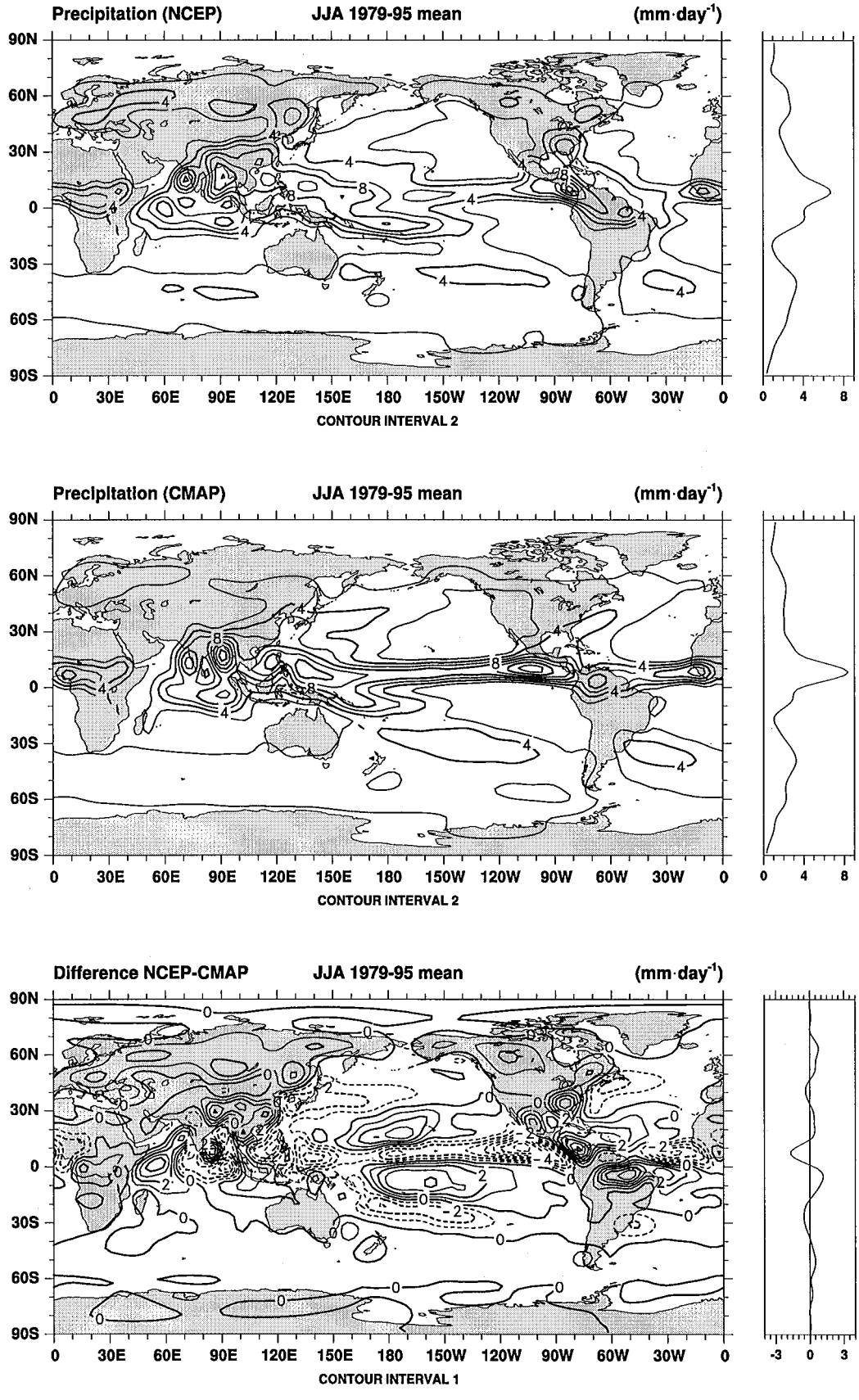

Fig. 7 Mean precipitation for June–July–August for the period 1979–1995 from the model, Xie–Arkin CMAP and their differences

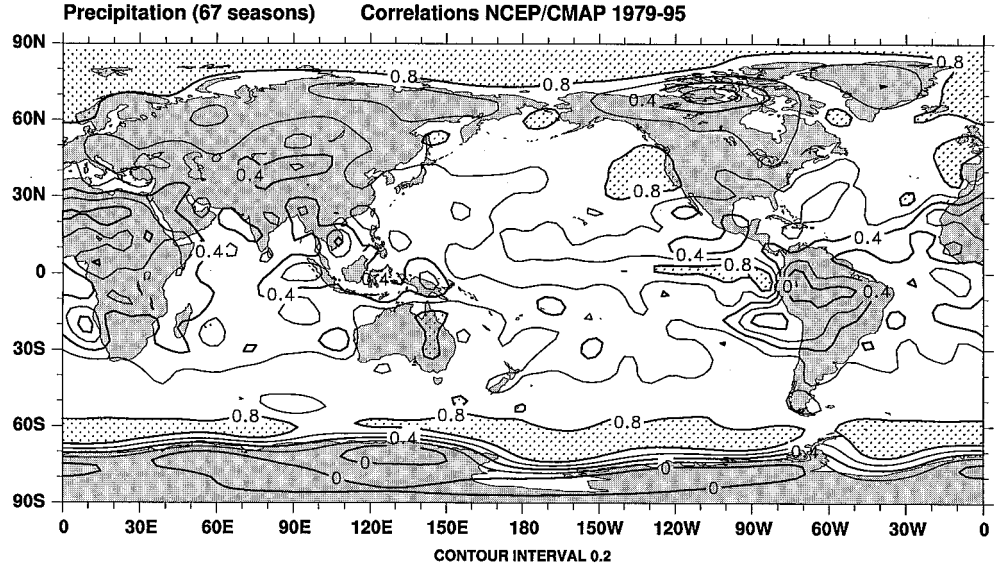

Fig. 8 Correlation coefficient between the seasonal anomalies in precipitation in NCEP and CMAP analyses over the period 1979 to 1995 (67 seasons). *Values* exceeding 0.8 are *stippled*

moisture budget balances given just the analyzed quantities. To some degree the values are smaller than anticipated, apparently indicating the dominance of the divergence field in shaping both products. Note that positive differences in Fig. 14 imply that the model E is too high, the model P is too low, and/or that the analyzed moisture divergence is too negative. Extensive efforts have been made to track down the analysis characteristics that lead to the features in Fig. 14. They appear to have multiple causes and examples of all three kinds of biases can be found. In retrospect, perhaps these differences are not so surprising as they highlight sources of systematic biases whether from the analyses or the model parametrizations.

Remarkably, many island stations show up as bull's-eyes in this difference field calculated from the model and the residual technique, and there are several other striking systematic differences that appear almost every month. Many features are strong and very consistent in all months, and their origin was quite puzzling. Each $E - P$ field by itself seems to be quite coherent and reasonable. Yet when differences are taken, bull's-eye features emerge centered almost over island stations throughout the global domain. The bull's-eyes arise from the moisture divergence, and can be partly seen also in the lower panel of Fig. 10. Also, they are found when computations are performed in both pressure and model coordinates. Attempts to trace the features to individual levels or layers were not very successful. At low levels, although identifiable, the features are quite ordinary and tend to be submerged in the overall field noise and interannual variability. The contributions to the bull's-eyes from about 300 to 400 mb emerge somewhat more clearly from the background noise but, as moisture amounts fall off substantially with height, their total contributions are not that large. So it is a systematic pattern with height from 1000 to 300 mb that separates these features from the noise which tends to cancel elsewhere as integrations are performed both in height and in time. It was determined that the primary term contributing to the bull's eyes is the eastward advection of moisture. Thus it emerges that the dominant contribution to the bull's-eye features comes from the eastward gradients in $\bar{q}$, arising from an almost imperceptible decrease in $\bar{q}$ at the station ($\frac{\partial \bar{q}}{\partial x}$ negative). Surprisingly, for the advection term, there is not a strong or systematic feature with reverse sign (i.e., a dipole structure). The implication is that at isolated island stations throughout the southern oceans, the model first guess in the vicinity is systematically slightly moister than the observed value, and the observed information is advected downstream affecting the analyzed values in that area. Consequently, the only feature emerging in the analyses is a bull's-eye slightly upstream from the station location.

Evidence for a dry bias in the upper tropospheric observations from certain rawinsondes, which include many of those identified in Fig. 14 with positive bull's-eyes, comes from the Soden and Lanzante (1996) study based upon upper tropospheric moisture from satellite-based water vapor channels. They find a negative bias in relative humidity as measured by the radiosondes with capacitive (e.g., Humicap) or carbon hygristor sensors of 10 to 20% in the upper troposphere. In the 1990s, many of the stations used Vaisala rawinsondes which feature the Humicap humidity sensor (e.g., at Marion and Gough Islands where the most distinctive bull's-eyes stand out). However, the comparison between the NCEP and NVAP precipitable water (e.g., Fig. 1) shows positive NCEP biases over most of the southern oceans of >2 mm although the biases are

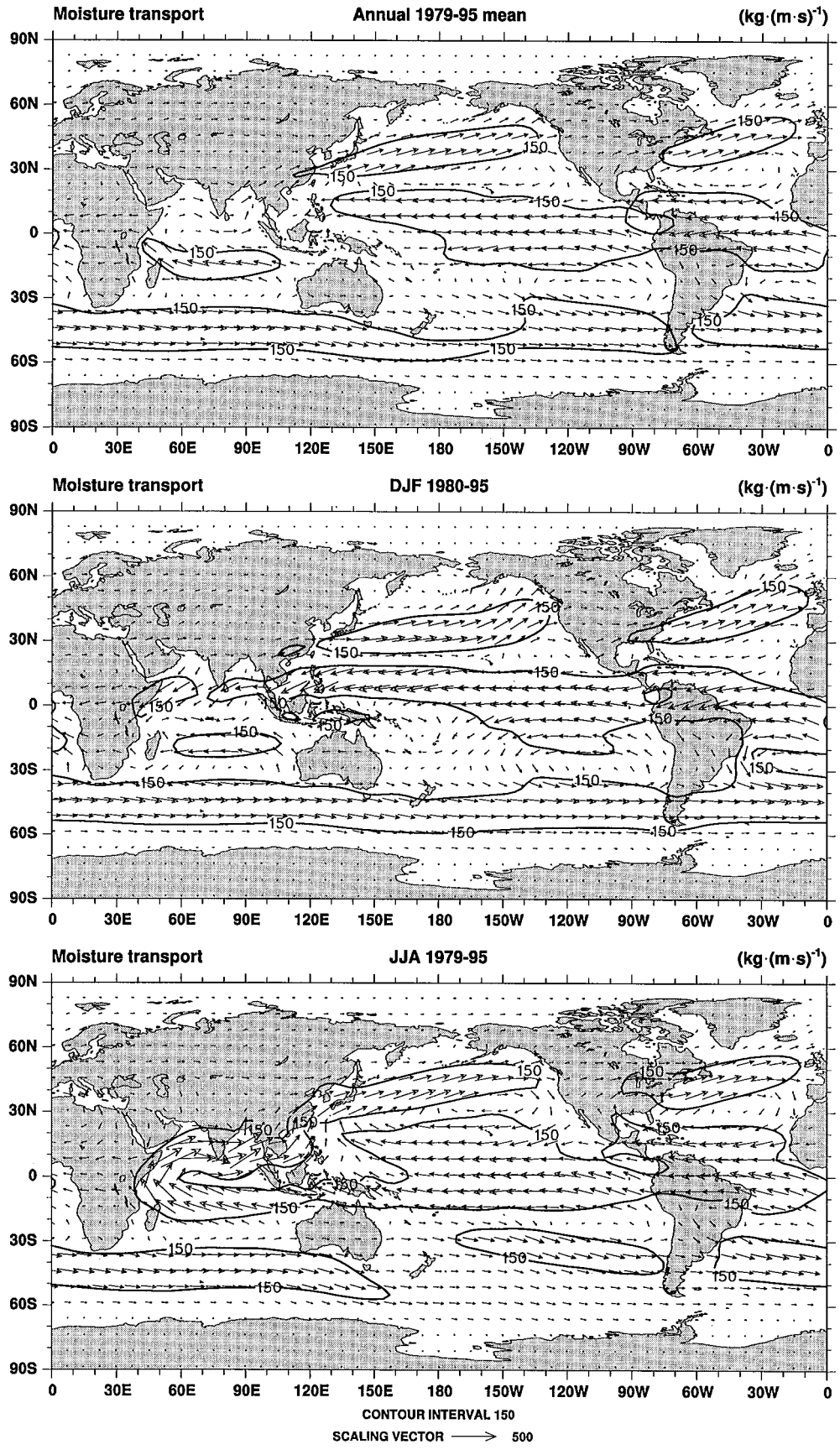

Fig. 9 The mean moisture transport for the period 1979–1995; annual, DJF and JJA

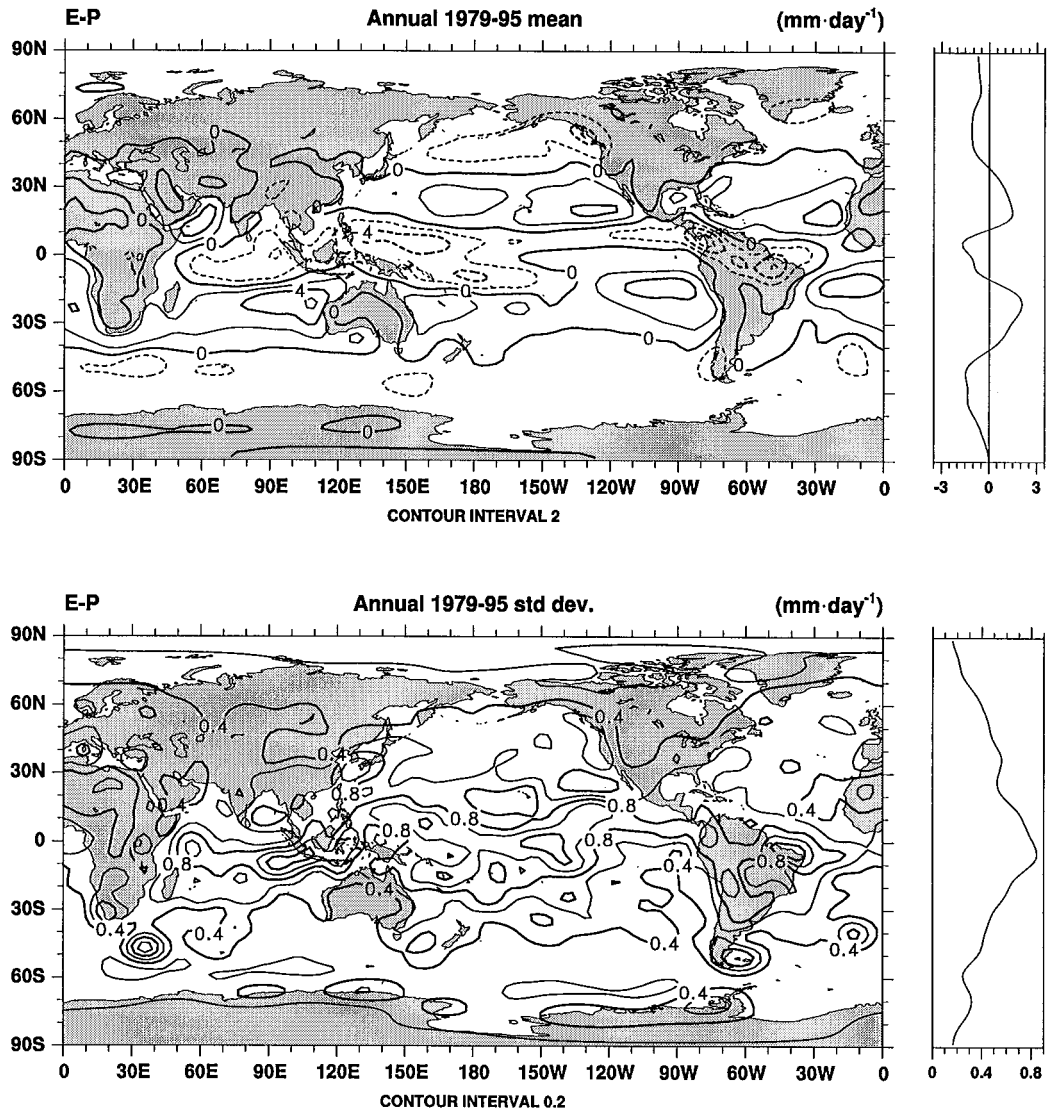

Fig. 10 Mean $E - P$ from the moisture budget for 1979–1995 derived as a residual from the indirect moisture budget computation; annual mean and annual standard deviation

slightly less than 2 mm at and just east of Marion and Gough. Therefore the evidence suggests that the problem arises mostly from the moist bias in the analyses over the open southern ocean.

A bull's-eye of reverse sign appears over Apia (Pago Pago) (14 °S 170 °W) which is an area where model precipitation is too high. Frequently other bull's-eyes occur nearby, for example a positive center near Penrhyn (9 °S 153 °W) and a negative center near Tahiti (17 °S 150 °W) (perhaps more associated with soundings in the Tuamotu Islands slightly farther east), and presumably these also relate to the characteristics of the different rawinsondes used, the biases in the analyzed moisture fields, and the model biases in precipitation and evaporation.

Other systematic features in Fig. 14 appear to have different origins that stem more from the model-generated fields of E and P. In particular, there are very sharp gradients in E across coastlines (Fig. 12), so that the feature south of Japan over the East China Sea appears to originate primarily from very strong E in the model, although there may also be insufficient model precipitation there. West of California, on the other hand, the positive feature stems from a deficiency in model P, as verified by the CMAP values. Over the southeastern part of the United States in northern summer, the bias originates from a systematic overestimate of P by the model, again as verified by CMAP (Fig. 7). These biases seem to extend to the Caribbean and Gulf of Mexico and also rainfall regions in the western tropical Pacific in the northern summer. The latter regional biases have also been found in earlier NMC models (Kanamitsu and Saha 1995, 1996) and in the NASA/Goddard reanalyses (Schubert et al. 1995).

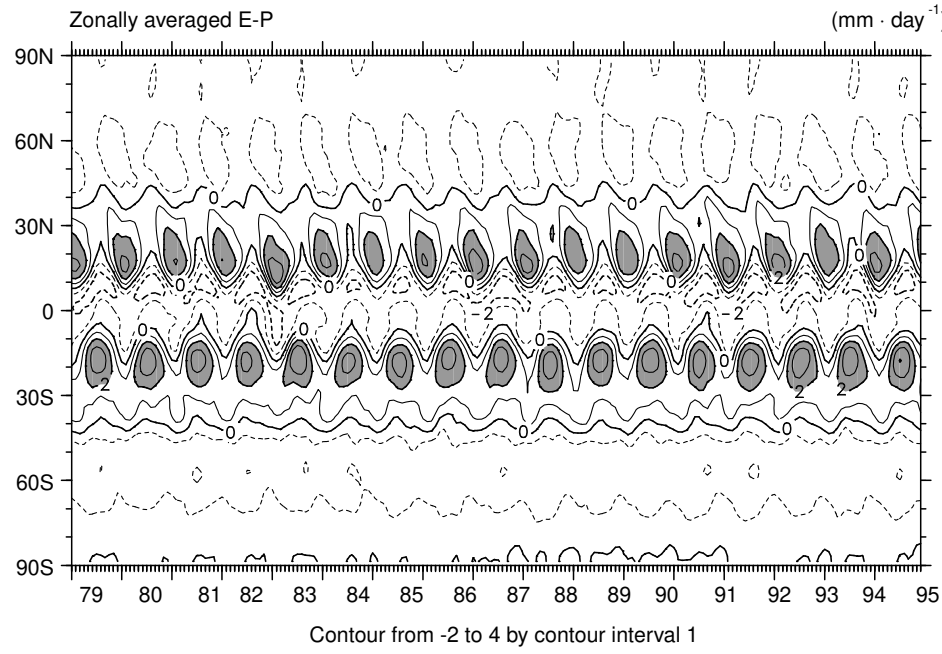

Fig. 11 Latitude-time series for the zonal averages of $E - P$. *Values* have been smoothed with a 1–2–1 weighting and *values* > 1 mm/day are *shaded*. *Negative values* are *dashed*

Many other features around the coast lines, such as the negative centers near 30 °E 30 °N and over Aden (42 °E 12 °N) and the positive center over Saudi Arabia, may be traceable to the presence of negative E in the model surrounding the Red Sea where values are large and positive, yet with a maximum in E over Saudi Arabia. In some places P is also negative, and these negative values of E and P presumably originate from ringing effects at finite spectral model resolution. The evaporation over Saudi Arabia appears to be excessive.

Over southern Africa, the tendency for positive values in Fig. 14 arises from errors in the moisture divergence. In June 1995 (not shown), for instance, model E and P estimates are very small (<1 mm/day) and $E - P \approx 0$, whereas the residual $E - P \approx -2$ mm/day implying excessive precipitation which does not verify from CMAP estimates.

Consequently, there are some places (such as North America and other areas where the precipitation is clearly wrong, or Saudi Arabia and the East China Sea where the evaporation seems to be at fault) where it appears that the residual method produces better answers, but in other places (such as southern Africa) the residual method estimates are clearly inferior to those from the model parametrizations. Both sets of estimates are affected by biases in moisture, as analyzed, while the moisture divergence depends critically on the velocity divergence field. The model estimates also depend upon the parametrizations of subgrid scale processes, such as convection, that influence E and P.

Therefore, while the comparison of $E - P$ from the moisture budget with the model result reveals similarities, there are also strong and systematic differences. In particular, the remarkable island station bull's-eyes are identified as originating from the moisture budget calculation through rather subtle effects arising from small but systematic differences in vertical moisture profiles from those in the surrounding oceans. In part this may reflect differences between radiosonde temperature and moisture amounts with either the model first guess or TOVS soundings. It indicates that the influence radius of rawinsonde moisture observations in the analyses, while perhaps appropriate for an individual sounding, is probably too small in the analyses of these data on average. Thus more attention needs to be given to biases in measurements of moisture at individual stations (for individual rawinsondes) and biases in the model.

4 Moisture budget sources of errors

A continuing major source of errors in the tropical moisture budget is the divergence field. The negative bias in precipitation in the NCEP reanalyses is perhaps an indication that the divergent circulation is too weak. Certainly the strength of the Hadley Circulation in the NCEP reanalyses is weaker than that of either the operational analyses from ECMWF and the ECMWF reanalyses. The critical dependence of the moisture budget on the veracity of the velocity field and,

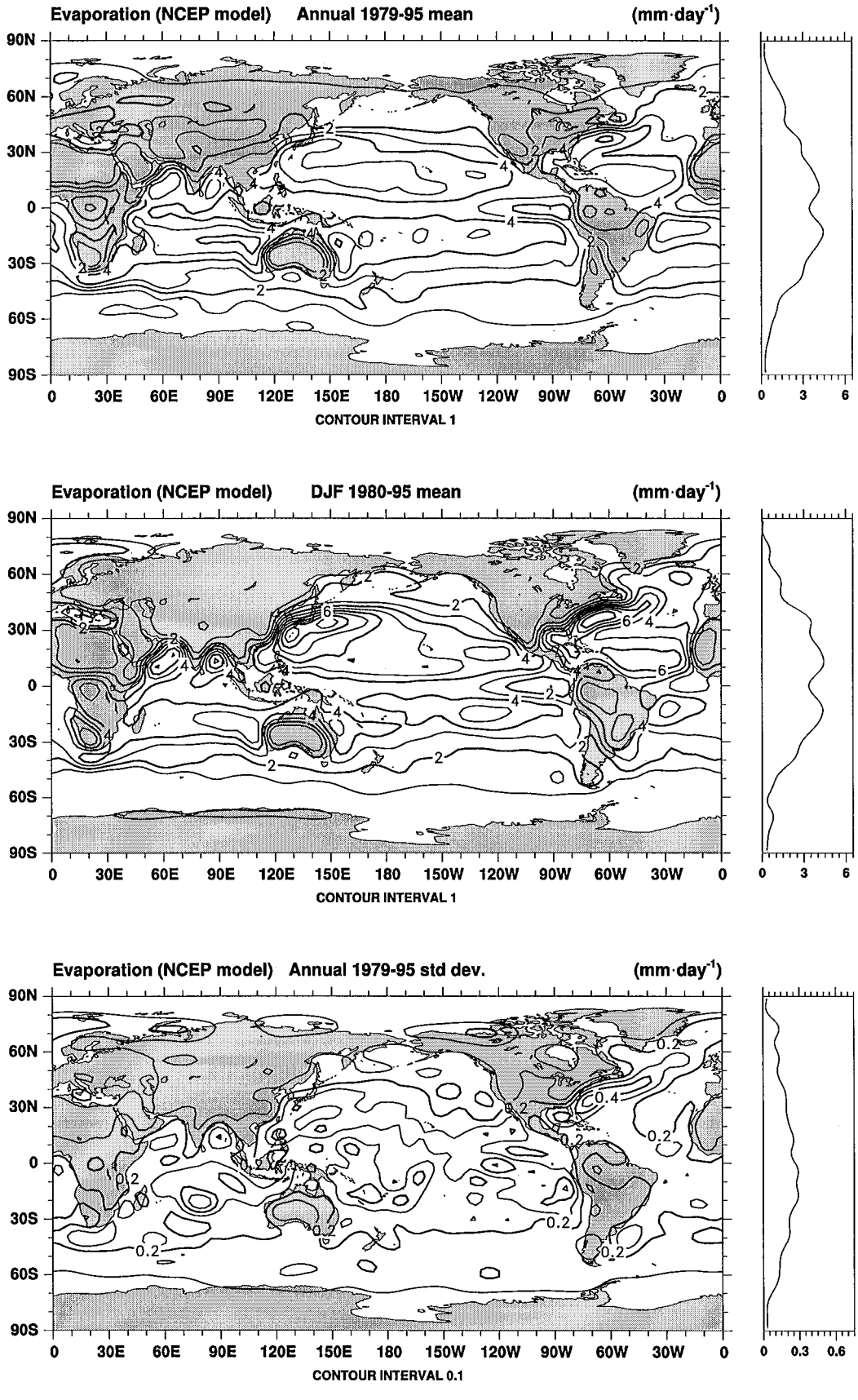

Fig. 12 Mean E for 1979–1995; annual, DJF, and the annual standard deviation

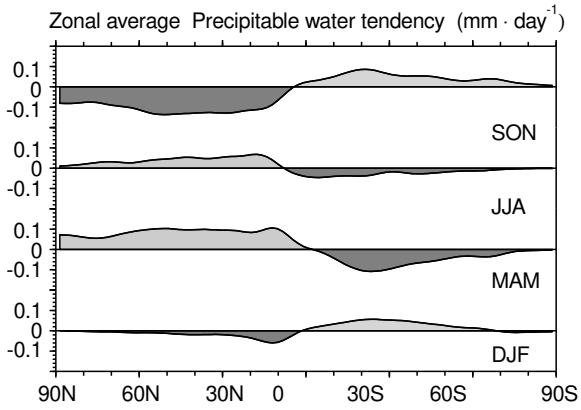

Fig. 13 Contribution of the mean precipitable water tendency to the moisture budget for each season DJF, MAM, JJA, SON

specifically, on the horizontal divergence in the tropics has been shown by Trenberth and Guillemot (1995). In midlatitudes, quasigeostrophic dynamics ensure that the divergence field is better known, and uncertainties in the moisture budget stem roughly equally from discrepancies in moisture analyses and the velocity field. It may be that improvements in this area will have to wait for global satellite-based wind measurements, although it seems that substantial progress should be possible if scatterometer winds at the surface were fully utilized in the analyses.

With 6-hourly analyses, the diurnal cycle errors are not a source of concern. However, mass imbalances are quite large in the NCEP reanalyses (Trenberth 1997) and can distort other budgets unless corrected for, although the impact is fairly small on the moisture budget. Vertical resolution can be an issue for analyses on pressure coordinates, but it is not a problem when use is made of all the levels in model coordinates, as done here. Horizontal resolution can be an issue where sharp gradients occur as there is evidence of spectral ringing and physically impossible values of negative precipitation and physically unlikely values of negative evaporation in the NCEP reanalyses. Horizontal resolution is also believed to be important in the vicinity of steep orography and associated low level diurnal jets (Helfand and Schubert 1995).

We have shown that substantial biases continue to exist in the moisture fields in the NCEP reanalyses. Information available from SSM/I is not utilized and nor are the water vapor channels of TOVS. At ECMWF and operationally at NCEP, brightness temperatures of the TOVS channels are now directly assimilated in place of retrievals and this apparently provides a substantial improvement in the depiction of moisture over the oceans. Nevertheless, it is apparent from the bull's-eyes in the $E - P$ difference fields, that there is difficulty in assimilating moisture into models and the information content inherent in these fields is not being adequately utilized. The moisture errors probably feed back and influence the divergent circulation through negative biases in latent heating arising from precipitation. Therefore this is one area where it seems possible to do a much better job and where it is extremely important to do so.

There are also other sources of moisture information not yet adequately utilized in the analyses including estimates of clouds and precipitation. Research is being pursued to assimilate this kind of information but parallel refinements of cloud algorithms and convective parametrizations are probably also required.

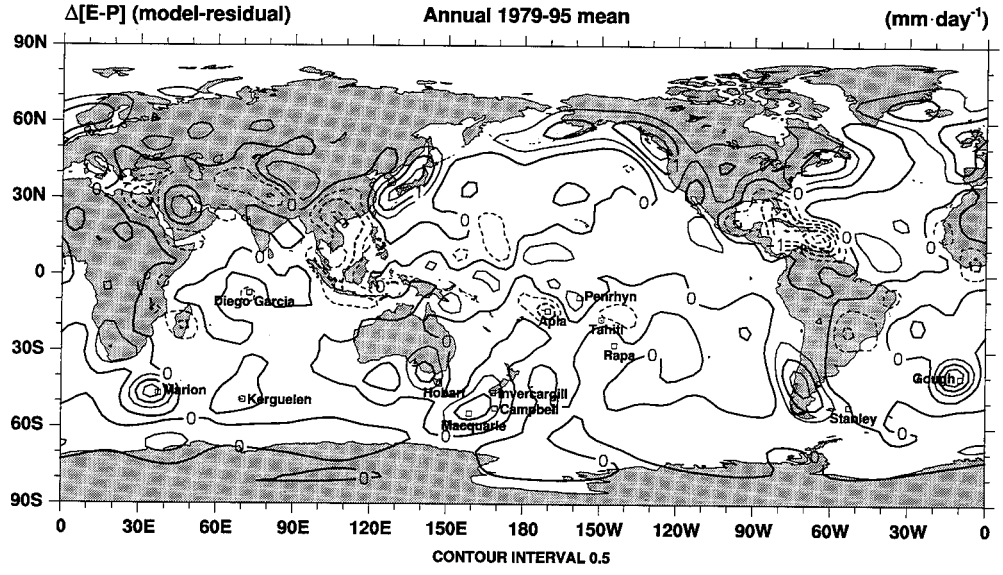

Fig. 14 Annual mean $\Delta(E - P)$ for 1979–1995 is the difference between the model E and P, and $E - P$ computed from the indirect budget method for the period 1979–1995. Some *island station locations* have been *identified*

It is apparent that there are errors arising in the precipitation field from the model physics. In the southeastern part of the United States in summer, the model is not able to sustain the observed high humidities giving rise to spurious precipitation (Kanamitsu and Saha 1995, 1996; Schubert et al. 1995). The same kind of error seems to occur in southeast Asia in summer. Errors in assigning soil moisture values or in the land surface moisture budget appear to be responsible for some errors in evaporation. We have shown the discrepancy that exists between the model $E - P$ and that from the residual technique, so that the moisture budget is not balanced in the analyses, a point made also by Mo and Higgins (1996). Improvements in parametrization of the moist physics in the model is an obvious need, and should pay off in improved forecasts as well.

5 Concluding remarks

Although the NCEP moisture-related quantities are useful for some purposes, it is apparent that there are substantial problems with these fields and the moisture budget is not balanced. The latter is not a surprising result as there is no constraint in the 4DDA to ensure moisture conservation, but it serves as a caution to unwary users of the analysis fields. Some problems are identified with the assimilating model physics, but several stem from the quality of the analyses. The latter certainly also depends on the assimilating model. We have shown that there are systematic differences between radiosonde moisture amounts and the analyses which presumably depend heavily on the model first guess in remote regions that show up as bull's-eyes in the $E - P$ difference fields. The implication is that the influence radius of rawinsonde moisture observations, which perhaps is appropriate for an individual sounding, is nevertheless too small in the analyses of these data on average. In addition, more attention needs to be given to biases in measurements of moisture from individual rawinsondes and the model first guess.

Substantial shortcomings mean that the analyses should be used with caution in climate and hydrological studies. The reanalyses are a great step forward for climate studies as they are in general much better than operational analyses in a number of ways, and in particular by being much more consistent in time and without the spurious changes associated with improvements in the 4DDA system. The strategy in reanalyses has always been that they should be done again, and indeed it is crucial that they be done again taking advantage of lessons learned and new developments. It is hoped that this work will help focus attention on the moisture budget and the scope for improvements in the analyses.

Acknowledgements This research is partly sponsored by NOAA under grant NA56GP0247 and by NASA under NASA Order No. W-18,077. Thanks go to Doug Lindholm who prepared all the data sets for use and Phil Arkin and Pingping Xie for the rainfall dataset. The National Center for Atmospheric Research (NCAR) is sponsored by the National Science Foundation.

References

Arkin PA, Xie P (1994) The Global Precipitation Climatology Project: First algorithm intercomparison project. Bull Am Meteorol Soc 75: 401–419

Chiu LS, Chang ATC, Janowiak J (1993) Comparison of monthly rain rates derived from GPI and SSM/I using probability distribution functions. J Appl Meteorol 32: 323–334

Gleckler PJ, Randall DA, Boer G, Colman R, Dix M, Galin V, Helfand M, Kiehl J, Kitoh A, Lau W, Liang X-Z, Lykossov V, McAvaney B, Miyakoda K, Planton S, Stern W (1995) Interpretation of ocean energy transports implied by atmospheric general circulation models. Geophys Res Lett 22: 791–794

Helfand HM, Schubert SD (1995) Climatology of the simulated Great Plains low-level jet and its contribution to the continental moisture budget of the United States. J Clim 8: 784–806

Huffman GJ, Adler RF, Arkin P, Chang A, Ferraro R, Gruber A, Janowiak J, McNab A, Rudolf B, Schneider U (1997) The Global Precipitation Climatology Project (GPCP) combined precipitation dataset. Bull Am Meteorol 78: 5–20

Hurrell JW, Trenberth KE (1996) Satellite versus surface estimates of air temperature since 1979. J Clim 9: 2222–2232

Jones PD (1994) Recent warming in global temperature series. Geophys Res Lett 21: 1149–1152

Kalnay E, Kanamitsu M, Kistler R, Collins W, Deaven D, Gandin L, Iredell M, Saha S, White G, Woollen J, Zhu Y, Chelliah M, Ebisuzaki W, Higgins W, Janowiak J, Mo K-C, Ropelewski C, Leetmaa A, Reynolds R, Jenne R (1996) The NCEP/NCAR Reanalysis Project. Bull Am Meteorol Soc 77: 437–471

Kanamitsu M, Saha S (1995) Spectral budget analysis of the short-range forecast error of the NMC medium-range forecast model. Mon Weather Rev 123: 1834–1850

Kanamitsu M, Saha S (1996) Systematic tendency error in budget calculations. Mon Weather Rev 124: 1145–1160

Legates DR, Willmott CJ (1990) Mean seasonal and spatial variability in gauge-corrected, global precipitation. Int J Climatol 10: 111–127

Liu WT, Tang W, Wentz F (1992) Precipitable water and surface humidity over global oceans from Special Sensor Microwave Imager and European Centre for Medium Range Weather Forecasts. J Geophys Res 97: 2251–2264

Mo K-C, Higgins RW (1996) Large-scale atmospheric moisture transport as evaluated in the NCEP/NCAR and the NASA/DAO reanalyses. J Clim 9: 1531–1545

Randel DL, Vonder Haar TH, Ringerud MA, Reinke DL, Stephens GL, Greenwald TJ, Combs CL (1996) A new global water vapor dataset. Bull Am Meteorol Soc 77: 1233–1246

Schubert S, Park C-K, Wu C-Y, Higgins W, Konratyeva Y, Molod A, Takacs L, Seablom M, Rood R (1995) A multiyear assimilation with GEOS-1 system: Overview and Results. Vol 6 NASA Tech Mem 104606. Tech Rep Ser on Global Modeling and Data Assimilation, Suarez M (ed): 182 pp

Soden BJ, Lanzante JR (1996) An assessment of satellite and radiosonde climatologies of upper tropospheric water vapor. J Clim 9: 1235–1250

Trenberth KE (1997) Using atmospheric budgets as a constraint on surface fluxes. J Clim 10: 1081–1096

Trenberth KE, Guillemot CJ (1995) Evaluation of the global atmospheric moisture budget as seen from analyses. J Clim 8: 2255–2272

Trenberth KE, Guillemot CJ (1996) Evaluation of the atmospheric moisture and hydrological cycle in the NCEP reanalyses. NCAR Technical Note NCAR/TN-430+STR, 300 pp

Trenberth KE, Solomon A (1994) The global heat balance: heat transports in the atmosphere and ocean. Clim Dyn 10: 107–134

Wittmeyer IL, Vonder Haar TH (1994) Analysis of the global ISCCP TOVS water vapor climatology. J Clim 7: 325–333

Xie P, Arkin PA (1996) Analysis of global monthly precipitation using gauge observations, satellite estimates and numerical model predictions J Clim 9: 840–858

Xie P, Arkin PA (1997) Global precipitation: A 17 year monthly analysis based on gauge observations, satellite estimates and numerical model outputs. Bull Am Meteor Soc 78: 2539–2558